Skeletal Radiol (2011) 40:1363–1368
DOI 10.1007/s00256-011-1160-0

CASE REPORT

Extrarenal rhabdoid tumor mimicking a sacral peripheral nerve sheath tumor

Matthew D. Dobbs · Hernan Correa · Herbert S. Schwartz · J. Herman Kan

Received: 20 January 2011 / Revised: 17 March 2011 / Accepted: 20 March 2011 / Published online: 9 April 2011

Abstract Extrarenal rhabdoid tumor is a rare, highly aggressive tumor of childhood with a poor prognosis. It represents <1% of pediatric soft tissue malignancies, typically involving infants. Frequently involved extrarenal sites include deep locations of the neck, abdomen, and paraspinal regions. The presence of "rhabdoid" cells is the characteristic histologic feature. Recent discovery of a specific genetic mutation enables a more accurate diagnosis. We present a case in an adolescent of extrarenal rhabdoid tumor arising within the sacral canal. This appears to be the first reported case of an extrarenal rhabdoid tumor arising within the sacral canal and mimicking a peripheral nerve sheath tumor. While rare, this tumor can be included in the radiologic differential diagnosis of peripheral nerve sheath tumors in children.

Keywords Rhabdoid tumor · Sarcoma · Sacrum · Malignant peripheral nerve sheath tumor · CT · MRI

M. D. Dobbs (✉) · J. H. Kan
Department of Radiology and Radiological Sciences,
Vanderbilt University Medical Center,
1161 Medical Center Dr, MCN CCC-1106,
Nashville, TN 37232–2675, USA
e-mail: matthew.dobbs@vanderbilt.edu

J. H. Kan
e-mail: herman.kan@vanderbilt.edu

H. Correa
Department of Pathology, Vanderbilt Children's Hospital,
1161 21st Ave South CC3322 MCN,
Nashville, TN 37232–2561, USA
e-mail: hernan.correa@vanderbilt.edu

H. S. Schwartz
Department of Orthopedic Oncology,
Vanderbilt University Medical Center,
Suite 4200, South Tower, MCE 1215 21st Ave South,
Nashville, TN 37232, USA
e-mail: herbert.s.schwartz@vanderbilt.edu

Introduction

Malignant rhabdoid tumors are classically found in the kidneys of children. Concomitant central nervous system (CNS) involvement in 10–20% of these patients was originally described in a large pathologic series of Wilms tumors [1, 2]. Extrarenal rhabdoid tumors are a rare subtype of soft tissue tumors with an extremely poor prognosis. Reported extrarenal sites include liver, heart, abdomen, neck, and paraspinal regions [3].

To our knowledge, the few case reports and series describing these tumors have not reported a case involving the sacral canal with neural foraminal involvement mimicking a nerve sheath tumor [4–6]. To our knowledge, this is the first reported case of extrarenal rhabdoid tumor involving the sacral canal and neural foramen. Pathologic analysis was critical in arriving at the final correct diagnosis in this case. Our case was unique in that it mimicked a malignant peripheral nerve sheath tumor (MPNST) by imaging.

Case report

A 17-year-old female presented with a 3-month history of left lower extremity pain and parasthesia extending down the back of her leg to the lateral foot and ankle (S1 distribution). Initial MRI demonstrated an enhancing T2 hyperintense mass arising from the left presacral space and contiguous with the left S2 neural foramen with bony remodeling and expansion of the foramen measuring 35 × 44 × 40 mm (Fig. 1). MRI of the brain and spine did not reveal any other lesions to support the preliminary clinical diagnosis of neurofibromatosis.

Follow-up MRI 7 months after the initial study revealed a 69 × 73 × 98 mm mass, predominantly isointense on T1

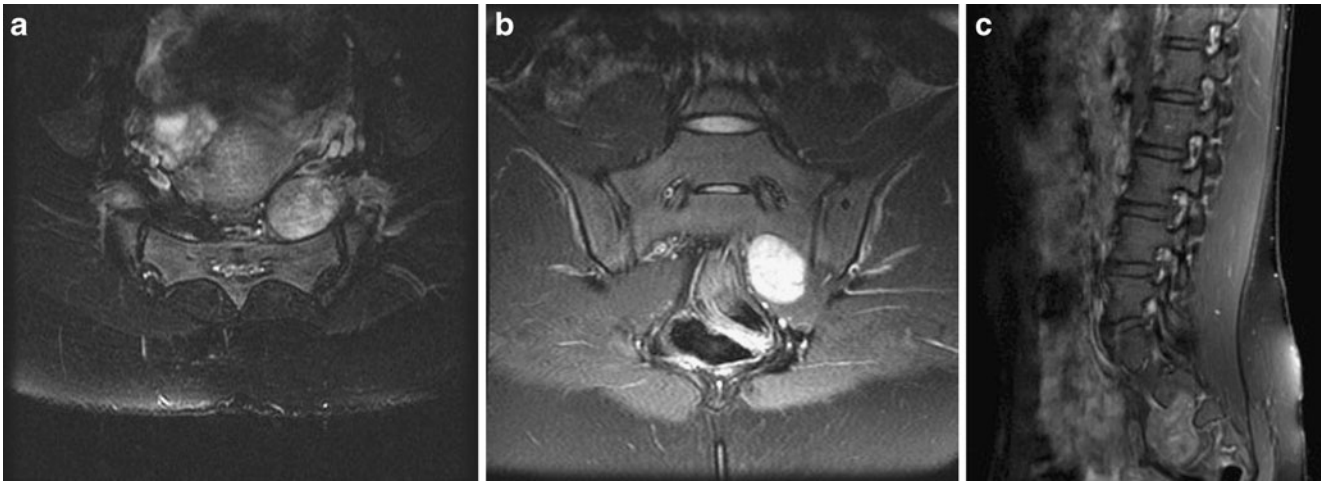

Fig. 1 Pelvic MR imaging at presentation. **a**, **b** Axial and coronal T2WI with fat suppression demonstrates 35 × 44 × 40 mm mass in left presacral space. **c** Sagittal T1WI with fat suppression post gadolinium demonstrates enhancing mass arising from left S2 neural foramen and extending into presacral space without invasion into adjacent bone

with areas of T1 hyperintensity, and heterogeneous yet predominantly T2 hyperintense signal, with avid contrast enhancement (Figs. 2, 3, 4, 5, 6, 7, 8). There was no surrounding osseous invasion. Denervation atrophy and myositis were noted in the left gluteal muscles (Fig. 2). The radiologic diagnosis was malignant peripheral nerve sheath tumor. CT of the chest, abdomen, and pelvis revealed the mass with bony remodeling of the sacrum and the left S2 foramen (Fig. 9) with no evidence of metastatic disease elsewhere. Both kidneys were normal without evidence of tumor. ^{18}F-FDG PET-CT demonstrated an intensely FDG avid sacral mass with no evidence of metastases (Fig. 10).

Pathologic analysis

CT-guided needle biopsy produced scant tissue consisting of undifferentiated cells with high nuclear-to-cytoplasmic ratio and hyperchromatic nuclei with small nucleoli. Rare cells with a small amount of eccentric, eosinophilic cytoplasm suggestive of rhabdoid cells were present. Scant mitoses were identified, and geographic areas of necrosis were present. The initial immunoperoxidase stain profile revealed positive membrane staining for CD99, and negative staining for myogenin, desmin, S-100, cytokeratin AE1/3, epithelial membrane antigen, and leukocyte common antigen. No tissue remained for additional immunohistochemical workup. With this initial battery of stains, the initial pathology interpretation was of a poorly differentiated neoplasm with features of Ewing sarcoma.

The second surgical biopsy of the left S2 lamina demonstrated sheets of cells with large, vesicular round to reniform nuclei with prominent central nucleoli. Rare cells exhibited the characteristic eccentric eosinophilic cytoplasm. Mitoses were frequent (9 in 10 high power fields) (Fig. 11). Foci of necrosis were also present. The immunohistochemical profile showed positive membrane staining for CD99, and negative staining of the tumor cells

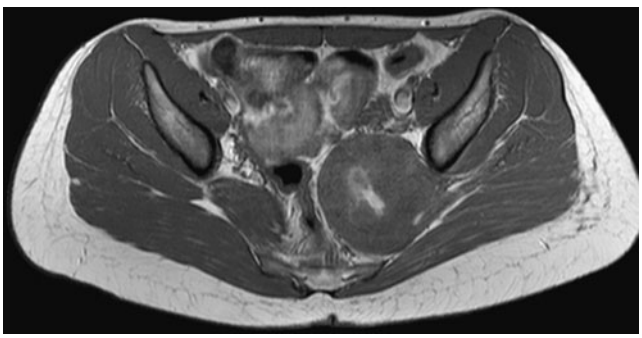

Fig. 2 Axial T1WI of the pelvis demonstrates predominant signal of the mass in the left pelvis to be isointense to muscle. Areas of hyperintensity in the center of the mass could be fat, protein, melanin, or hemorrhage. Note fatty infiltration of gluteus maximus and medius on the left

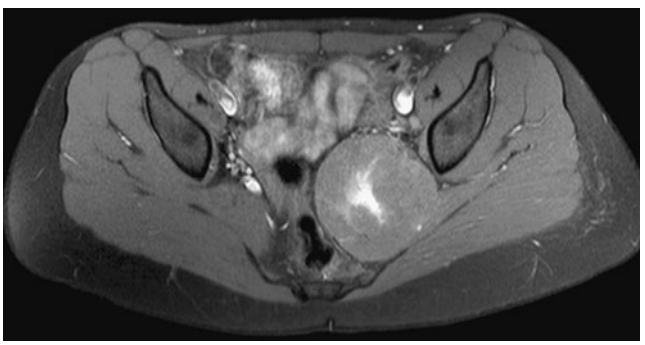

Fig. 3 Axial PDWI with fat suppression shows a heterogeneous pelvic mass. The areas of hyperintensity in the center of the mass do not suppress with fat suppression, suggesting hemorrhagic or proteinaceous material

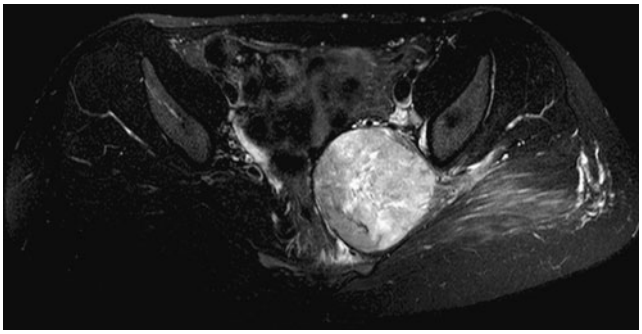

Fig. 4 Axial T2WI with fat suppression shows a predominantly hyperintense large left pelvic mass. Also note increased signal within the left gluteal muscles representing denervation atrophy

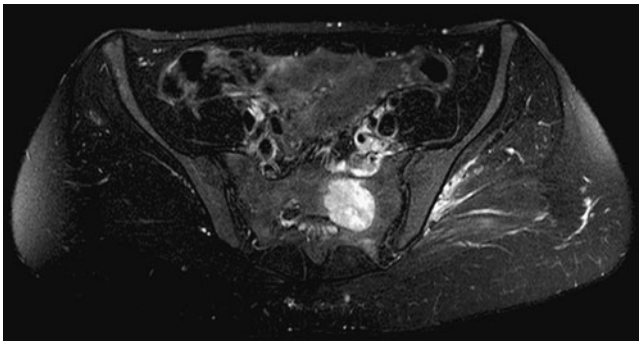

Fig. 5 Axial T2WI with fat suppression shows a predominantly hyperintense mass within an expanded left S2 sacral foramen. Note that surrounding bone has no marrow edema to suggest surrounding osseous invasion

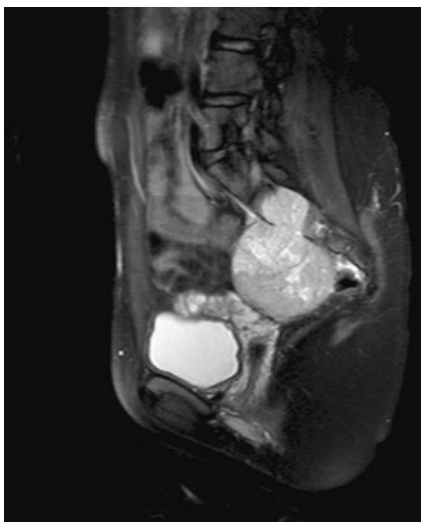

Fig. 6 Sagittal T2WI with fat suppression demonstrates a heterogeneous hyperintense mass arising from the sacral canal, exiting via the S2 foramen, and having a large presacral component

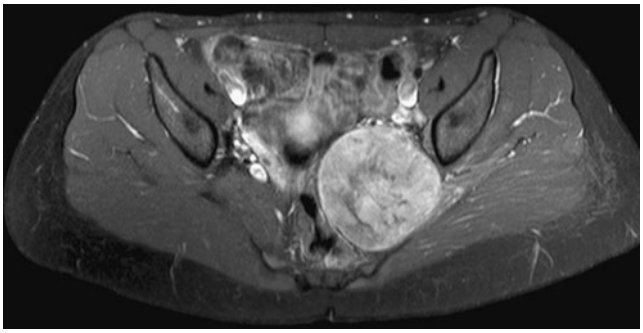

Fig. 7 Axial T1WI+gadolinium with fat suppression demonstrates an avidly enhancing mass with heterogeneity in the left presacral region. The mass is well-encapsulated with no surrounding enhancement

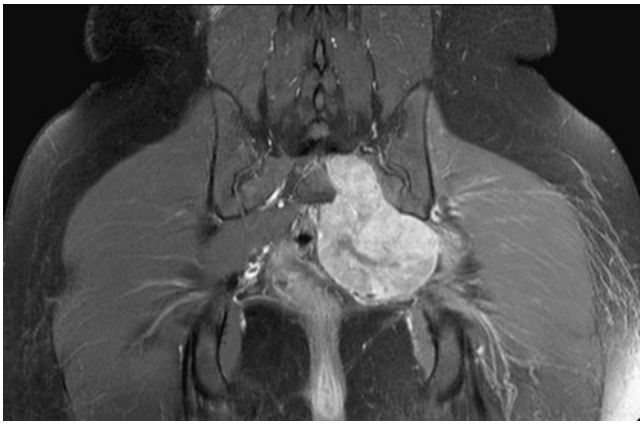

Fig. 8 Coronal T1WI+gadolinium with fat suppression shows an enhancing mass in the sacral canal, exiting an enlarged S2 foramen, with the largest portion in the presacral region

Fig. 9 Unenhanced CT of the pelvis demonstrates smooth bone remodeling of the left S2 sacral foramen filled with soft tissue. Smooth bone remodeling suggests a slow growing process

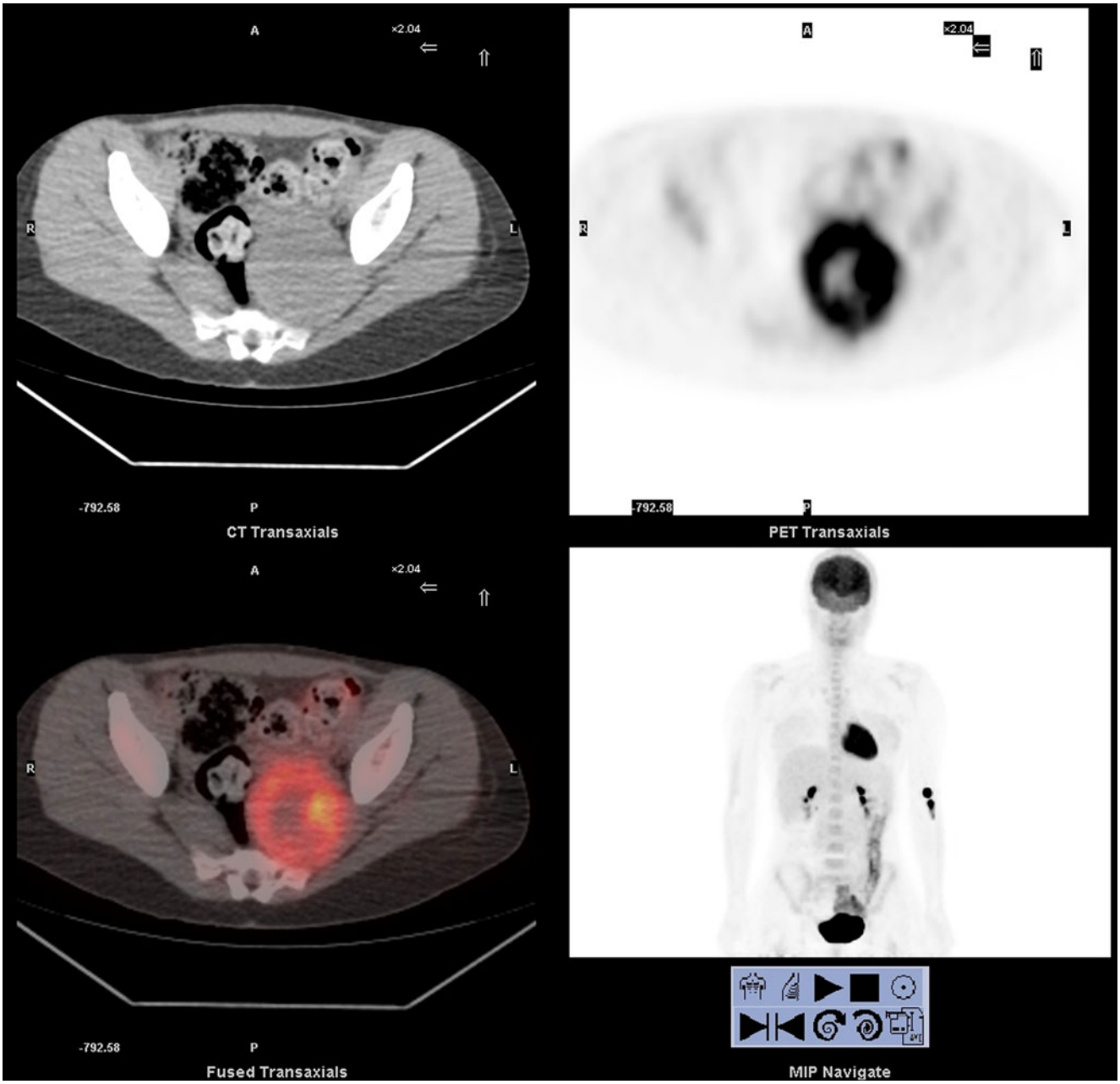

Fig. 10 Composite image from ^{18}F-FDG PET-CT shows an intensely FDG-avid presacral mass consistent with malignancy. Central non-FDG-avid region represents central necrosis

for INI-1, synaptophysin, neuron-specific enolase, chromogranin, cytokeratins CK19, smooth muscle actin, muscle-specific actin, WT-1, p53, and HMB45. The electron microscopy analysis showed a primitive neoplasm with closely apposed cells with rare primitive cell junctions but no true desmosomes. In addition, a striking feature in some cells is the presence of cytoplasmic aggregates of intermediate filaments, indicative of rhabdoid features [7].

Conventional cytogenetic studies revealed the presence of a hypodiploid clone characterized by gain of chromosome 8, loss of chromosome 10, and a derivative isodicentric chromosome comprised of the long arms of chromosome 22 with an interstitial deletion at band 22q11.2 in one arm. FISH studies for SYT (18q11.2) and EWS (22q12) rearrangements were negative.

The karyotypic hallmark of renal and extrarenal rhabdoid tumor is loss of chromosome 22 or partial deletion of the long arm of chromosome 22, particularly the *INI1* gene region at 22q11.2 [8–10].

The patient received carboplatin, cyclophosphamide, and etoposideneoadjuvant chemotherapy, followed by marginal resection of a 10 × 9 × 2.5 cm mass to alleviate the intense

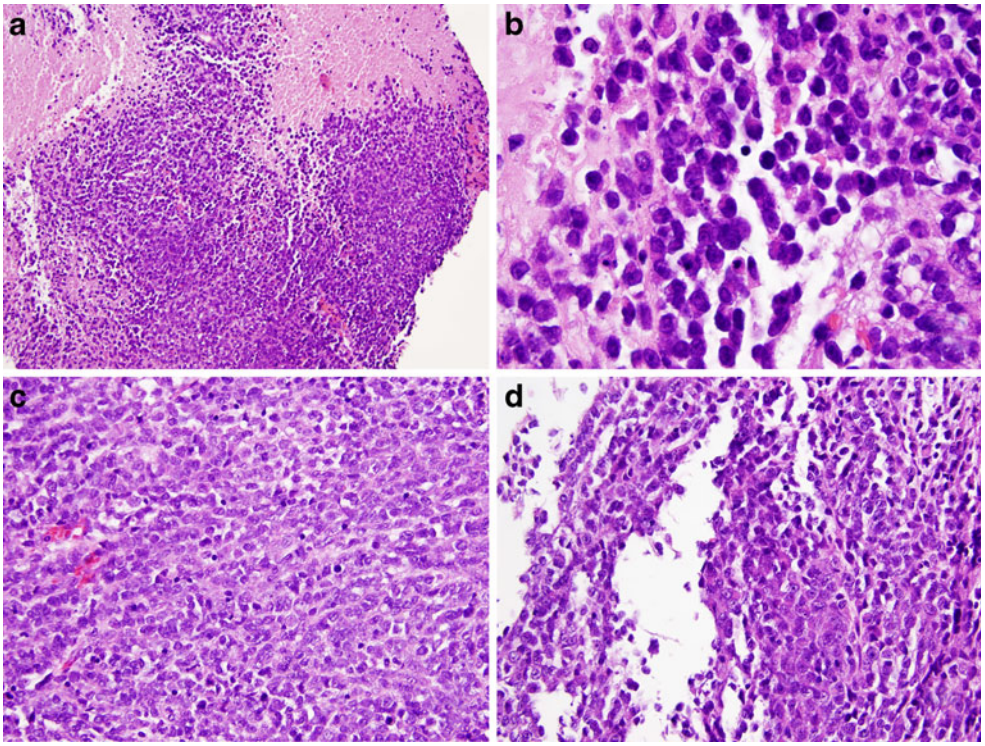

Fig. 11 Micrograph of hematoxylin and eosin (H&E)-stained slides present sheets of cells with large, vesicular round to reniform nuclei with prominent central nucleoli. Rare cells exhibit the characteristic eccentric eosinophilic cytoplasm

neuropathic pain. Histologically, the post-therapy tumor exhibited a diffusely infiltrative tumor with extensive perineural invasion, and focal vascular invasion by viable tumor cells. The tumor cells infiltrated the surrounding soft tissue in nests, cords, and as single cells, reaching the surgical margins. They had the same undifferentiated appearance with rare rhabdoid cells as in the original biopsies plus frequent mitoses (9/10 HPF). There was central necrosis, involving less than 30% of the tumor.

Discussion

Rhabdoid tumors were originally termed "rhabdomyosarcomatoid tumor" due to their similar appearance to muscle-based tumors [11]. Originally described as a very aggressive childhood renal neoplasm in the original 1970's Wilms tumor study, it has since been categorized separately from Wilms and rhabdomyosarcoma [1, 12]. Extrarenal rhabdoid tumors are rare tumors that occur outside of the kidney. Prior series and case reports have reported cervical neural foramen as well as paraspinal involvement in the absence of a primary lesion arising from the kidney [4–6]. To our knowledge, our study is the first case of a child with a primary rhabdoid tumor of the sacral neural foramen in the absence of a renal primary or CNS primary, radiologically mimicking a malignant peripheral nerve sheath tumor.

From the histopathology perspective, rhabdoid cells are known to occur in a variety of tumors, including carcinomas, sarcomas, meningiomas, melanomas, and mesotheliomas [3, 13, 14].

Extrarenal rhabdoid tumors characteristically have mutations or homozygous deletions of the *INI1* (*hSNF5* or *SMARCB1*) gene located on chromosome 22 band q11.2. Therefore, absent immunohistochemical staining for INI-1 is demonstrated in nearly all malignant rhabdoid tumors, regardless of location, and is a highly sensitive and specific diagnostic tool [3, 7, 14, 15].

The radiology differential diagnosis of a mass in this location includes neurofibroma, schwannoma, ganglioneuroma, paraganglioma, meningioma, perineural cyst, malignant peripheral nerve sheath tumor, and soft tissue sarcoma. A perineural cyst would have fluid signal intensity and would not show contrast enhancement. The mass appeared to arise from the sacral nerve trunk because there was expansion of the sacral neural canal and thickening of the cephalad sacral nerve root, and we were unable to separate the nerve from the mass. A non-neural-based tumor would be less likely to show thickening of the sacral nerve, and the nerve would likely be able to be identified separately from the mass (in our case there appeared to be fusiform expansion of the nerve).

Although the sacral erosion suggested that the mass must have been present for some time, the lesion lacked some of the other signs of benign nerve sheath tumors such as the "target sign," "split-fat sign," and "fascicular sign" [16, 17]. There was also avid contrast enhancement, central necrosis on PET-CT, internal heterogeneity including hemorrhage,

marked interval enlargement, and denervation edema in the left gluteal muscles, all features that indicated malignancy.

Pathologic differential diagnosis includes Ewing sarcoma, malignant peripheral nerve sheath tumor, rhabdomyosarcoma, and synovial sarcoma. Lymphoma and melanoma were also considered as a remote possibility. The positive membrane staining for CD99 may lead to an incorrect diagnosis of Ewing sarcoma if no additional work-up is performed, including further immunoperoxidase stains and genetic studies. In our case, the FISH analysis for EWS-FLI-1 and EWS-ERG translocations were negative, making Ewing sarcoma unlikely. After sufficient material was obtained for additional workup, absent staining for INI-1 was demonstrated, and genetic confirmation was achieved by the finding of the deletion involving 22q11.2, an unequivocal diagnosis of extrarenal rhabdoid tumor was reached. This point underscores the need to plan for obtaining an adequate sample for complete pathologic evaluation.

In conclusion, we have presented the first reported case of a primary extrarenal rhabdoid tumor with sacral neural foramen involvement. Our case mimicked a nerve sheath tumor by imaging, with MPNST the most favored prospective diagnosis. The pathologic analysis with immunohistochemical staining for INI-1 and genetic testing for abnormalities in chromosome 22 band q11.2 was integral in the final diagnosis. While rare, extrarenal rhabdoid tumor may be included in the radiologic differential diagnosis of paraspinal peripheral nerve sheath tumors.

Funding/disclosures/conflicts of interest None.

References

1. Beckwith JB, Palmer NF. Histopathology and prognosis of Wilms tumors: results from the First National Wilms' Tumor Study. Cancer. 1978;41(5):1937–48.
2. Wagner L, Hill DA, Fuller C, Pedrosa M, Bhakta M, Perry A, et al. Treatment of metastatic rhabdoid tumor of the kidney. J Pediatr Hematol Oncol. 2002;24(5):385–8.
3. Oda Y, Tsuneyoshi M. Extrarenal rhabdoid tumors of soft tissue: clinicopathological and molecular genetic review and distinction from other soft-tissue sarcomas with rhabdoid features. Pathol Int. 2006;56(6):287–95.
4. Robbens C, Vanwyck R, Wilms G, Sciot R, Debiec-Rychter M. An extrarenal rhabdoid tumor of the cervical spine with bony involvement. Skeletal Radiol. 2007;36(4):341–5.
5. Garces-Inigo EF, Leung R, Sebire NJ, McHugh K. Extrarenal rhabdoid tumours outside the central nervous system in infancy. Pediatr Radiol. 2009;39(8):817–22.
6. Bourdeaut F, Freneaux P, Thuille B, Bergeron C, Laurence V, Brugieres L, et al. Extra-renal non-cerebral rhabdoid tumours. Pediatr Blood Cancer. 2008;51(3):363–8.
7. Hoot AC, Russo P, Judkins AR, Perlman EJ, Biegel JA. Immunohistochemical analysis of hSNF5/INI1 distinguishes renal and extra-renal malignant rhabdoid tumors from other pediatric soft tissue tumors. Am J Surg Pathol. 2004;28(11):1485–91.
8. Biegel JA, Kalpana G, Knudsen ES, Packer RJ, Roberts CWM, Thiele CJ, et al. The role of INI1 and the SWI/SNF complex in the development of rhabdoid tumors: meeting summary from the workshop on childhood atypical teratoid/rhabdoid tumors. Cancer Res. 2002;62(1):323–8.
9. Biegel JA, Tan L, Zhang F, Wainwright L, Russo P, Rorke LB. Alterations of the hSNF5/INI1 gene in central nervous system atypical teratoid/rhabdoidtumors and renal and extrarenal rhabdoid tumors. Clin Cancer Res. 2002;8(11):3461–7.
10. Biegel JA, Zhou J-Y, Rorke LB, Stenstrom C, Wainwright LM, Fogelgren B. Germ-line and acquired mutations of INI1 in atypical teratoid and rhabdoid tumors. Cancer Res. 1999;59 (1):74–9.
11. Winger DI, Buyuk A, Bohrer S, Turi GK, Scimeca P, Price AP, et al. Radiology-pathology conference: rhabdoid tumor of the kidney. Clin Imaging. 2006;30(2):132–6.
12. Parham DM, Weeks DA, Beckwith JB. The clinicopathologic spectrum of putative extrarenal rhabdoid tumors. An analysis of 42 cases studied with immunohistochemistry or electron microscopy. Am J Surg Pathol. 1994;18(10):1010–29.
13. Guillou L, Wadden C, Coindre JM, Krausz T, Fletcher CD. "Proximal-type" epithelioid sarcoma, a distinctive aggressive neoplasm showing rhabdoid features. Clinicopathologic, immunohistochemical, and ultrastructural study of a series. Am J Surg Pathol. 1997;21(2):130–46.
14. Alaggio R, Boldrini R, Di Venosa B, Rosolen A, Bisogno G, Magro G. Pediatric extra-renal rhabdoid tumors with unusual morphology: a diagnostic pitfall for small biopsies. Pathol Res Pract. 2009;205(7):451–7.
15. Sigauke E, Rakheja D, Maddox DL, Hladik CL, White CL, Timmons CF, et al. Absence of expression of SMARCB1/INI1 in malignant rhabdoid tumors of the central nervous system, kidneys and soft tissue: an immunohistochemical study with implications for diagnosis. Mod Pathol. 2006;19(5):717–25.
16. Stull MA, Moser RP, Kransdorf MJ, Bogumill GP, Nelson MC. Magnetic resonance appearance of peripheral nerve sheath tumors. Skeletal Radiol. 1991;20:9–14.
17. Murphey MD, Smith WS, Smith SE, Kransdorf MJ, Temple HT. Imaging of musculoskeletal neurogenic tumors: radiologic-pathologic correlation. Radiographics. 1999;19:1253–80.